RSC Advances

ROYAL SOCIETY OF CHEMISTRY

www.rsc.org/advances

Magnetofluidic control of the breakup of ferrofluid droplets in a microfluidic Y-junction

Huajun Li, Yining Wu, Xiaoda Wang, Chunying Zhu*, Taotao Fu, Youguang Ma*

State Key Laboratory of Chemical Engineering, Collaborative Innovation Center of Chemical science and Engineering (Tianjin), School of Chemical Engineering and Technology, Tianjin University, Tianjin 300072, China

* Corresponding authors: zhchy971@tju.edu.cn (C. Zhu); ygma@tju.edu.cn (Y. Ma)

Abstract: This paper is mainly focused on the investigation of the magnetofluidic control of the breakup of ferrofluid droplets in a symmetric Y-junction. The asymmetric breakup of the ferrofluid droplet or non-breakup with filtering the mother droplet into a desired branch to separate it from the satellite droplet was implemented by an external magnetic field. The breakup processes of ferrofluid droplets with and without the magnetic field were studied systematically. The influences of both the flow rate ratio between the continuous phase and dispersed phase and the magnetic flux density on the sizes of daughter droplets were determined. It was found that the attractive magnetic force shifted the mass center of mother droplet in the upstream main channel, which accordingly facilitated the asymmetric breakup of the droplet at the downstream Y-junction. A power function correlation for precisely predicting the sizes of daughter droplets was proposed by introducing the magnetic Bond number (Bo_m). Moreover, we also found that the controllable magnetic force could promote the pattern transition between the breakup and non-breakup of ferrofluid droplets.

Keywords: Magnetofluidic, Ferrofluid droplet, Breakup, Magnetic field, microfluidic Y-junction

1 Introduction

In recent years, the rapid development of microfluidic devices has attracted increasing attention in industrial application and academic research with various advantages such as safety, high efficiency and controllability.[1-3] Meanwhile, microfluidics combining with magnetic particles as the micro-magnetofluidics has been widely applied in biological analysis, separation process, catalytic reaction and micropumps,[4-7] in which ferrofluid is actually a stable colloidal suspension of ferromagnetic nanoparticles with a diameter of 10 nanometers or less. Since the ferrofluid was discovered in the early 1960s, it has been used extensively in various research fields such as biology, medical treatment and chemical analysis.[8-11]

In the practical application, it is indispensable to precisely control the size of the ferrofluid droplet. The needful magnetic force depends primarily on the volume of the droplet and the magnetization intensity. The typical microfluidic configurations used to generate droplets include T-junction,[12] flow-focusing [13] and co-flowing.[14] In order to adjust the droplet size more flexibly and conveniently, extensive works have been conducted with external sources in the field of droplet generation. The external sources mainly include electric,[15] magnetic,[16] acoustic, [17] thermal [18] and pneumatic.[19]

In the applications of microfluidic devices, precisely tailoring droplets is usually needed to obtain the desirable sizes. The breakup of a mother droplet into two or more daughter droplets would be a potential approach. The breakup of droplets in the microfluidic device could be effectively adjusted by both passive and active manners. In the passive system, the breakup process and the sizes of the daughter droplets could be manipulated by altering the lengths of the branches,[20] adding obstacles [21] and introducing the "tuning flow" into the branch channels.[22] However, these methods often need either changing the channel structure or adding more sophisticated equipment and enable not to realize accurate controlling for each individual droplet. Compared to the rigid passive manner, active control could increase the robustness of the system and offer great flexibility in droplet manipulation. Link *et al*. [23] reported an electric control method for the breakup of charged droplets in a continuous-flow platform where the electric field was induced by indium tin oxide (ITO) electrodes. Yap *et al*. [24] utilized a thermal control technique for microdroplets at a T-bifurcation, the control concept is resulted from the temperature-sensitive fluidic resistance of the branches and the thermocapillary effect. Cheung and Qiu [25] utilized the acoustic stimulation to create periodic oscillation to control the sizes of droplets. Recently, the magnetic manipulation has attracted considerable attention.[11, 26, 27] In contrary to the manipulations by the electric field and temperature field, the interaction between the magnetism and fluid flow provides a truly wireless approach for the droplet manipulation that is not affected by heat, pH level or ion concentration. [26] Moreover,

most of the applications of the magnetic field are not restricted by the channel structure.[27]

In general, the external magnetic force is mainly induced by the permanent magnet and the electromagnet. [16, 28, 29] Nguyen *et al*. [28] conducted and controlled the droplet motion by changing the electric current in the array of planar coils. Say-Hwa *et al*. [29] investigated the influence of the position of the magnet on the formation of ferrofluid droplets at a microfluidic T-junction. When the magnet was placed upstream of the T-junction, the magnetic force delayed the breakup process and formed bigger droplets. On the contrary, smaller droplets would be formed. Liu *et al*. [9] studied the influences of both uniform and non-uniform magnetic fields on the formation of ferrofluid droplets in the flow-focusing configuration. Both numerical and experimental investigations showed that the change in the droplet size depended on the fluid flow rates and the magnetic flux density. The similar observations were achieved by Tan and Nguyen [30] and Wu *et al*..[16] More recently, Wu *et al*. [31] investigated the breakup dynamics of the ferrofluid droplet under magnetic fields in a microfluidic T-junction. It was found that the breakup regime could be varied by the uniform magnetic field, and the non-uniform magnetic field could realize the asymmetric breakup of ferrofluid droplets. However, in Wu's experiment, the operating range of capillary number is very narrow and accurate magnetic control over the droplet size needs to be further deeply studied. To our best knowledge, few studies were focused on the breakup of ferrofluid droplets, and most of existing

investigations were carried out in the T-junction and flow-focusing junction, while similar study in the usually used microfluidic Y-junction [22, 32, 33] has not been reported. Therefore, the breakup processes of ferrofluid droplets in a microfluidic Y-junction with and without the magnetic field were systematically studied. The influences of both the flow rate ratio between the continuous phase and dispersed phase and the magnetic effect on the droplet size were investigated experimentally. We expect that this study could provide an effective method to actively control the breakup of ferrofluid droplets and generate the ferrofluid emulsions of predetermine sizes.

2 Experimental

2.1 Details of microchannel

The layout of the microchannel is shown in Figure 1, which consists of a cross-flowing T-junction to form droplets and a square loop. The dispersed phase (ferrofluid) flows into the junction at a flow rate of Q_d, and the continuous phase (mineral oil) flows into the main channel with the flow rate of Q_c. These two flow streams converged at the T-junction downstream to form new droplets. In the downstream along the T-junction, the microchannel splits into two identical arms at a Y-junction divergence where the droplet could break or simply enter into one of the arms. Subsequently the two streams recombined and exited into the outlet channel. The microfluidic device was fabricated in a plate (100 × 60 × 8 mm) of polymethyl methacrylate (PMMA) by precision milling and sealed with an equirotal PMMA plate. The microchannel has a square cross-section of 400 μm wide and 400 μm high.

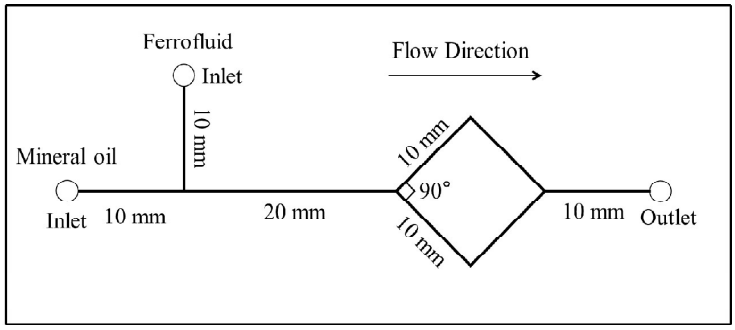

Fig.1 Schematic diagram of the microfluidic channel. The ferrofluid droplet is formed in a microfluidic T-junction and split into two daughter droplets at the symmetric Y-junction divergence. The cross-section of the microchannel is 400 μm (width) × 400 μm (height).

2.2 Experimental setup and methods

The scheme of the experimental setup is shown in Figure 2. The microfluidic device was placed above an inverted microscope connecting to a high-speed camera (MotionPro Y5, IDT, USA). A cold fiber illumination (Philips 13629, Philips, Japan) was placed on the top of microchannel as the working light source. The dispersed phase and the continuous phase were injected to the microchannel from two independent syringes driven by syringe pumps (Harvard Apparatus, PHD 22/2000, USA). The non-uniform magnetic field was realized by placing the neodymium iron boron (NdFeB) magnet (50 × 15 × 15 mm) at one side of the square loop. The Y-junction divergence where the droplets broke up was placed in the same height with the center of the magnet. The magnetization direction was perpendicular to the main straight channel. The magnetization of the fluid interacts with the external magnetic field could create an attractive body force on the ferrofluid per unit volume [29]:

$$F_m = \mu_0 M \nabla H \quad (1)$$

where μ_0 is the magnetic permeability of free space, $\mu_0 = 4\pi \times 10^{-7}$ N/A^2, M is the intensity of magnetization and ∇H is the gradient of the magnetic field strength. Figure 3 illustrates the magnetization curve for the ferrofluid used in our experiments (EMG 807, Ferrotech, USA). It could be clearly found from Fig. 3 that the effect the magnetic field on the magnetization of the ferrofluid is quite sensitive as long as it is below the saturation point, even if a considerably small magnetic field. The magnetic flux density and the magnetic gradient could be easily adjusted by changing the distance between the ferrofluid and the magnet, as shown in Figure 4. The magnetic flux density at the Y-junction divergence was measured using a gaussmeter (TM701, Kanetec, Japan) with an accuracy of 0.01 mT. The droplet size and velocity were processed by customized image processing software (MATLAB, MathWorks).

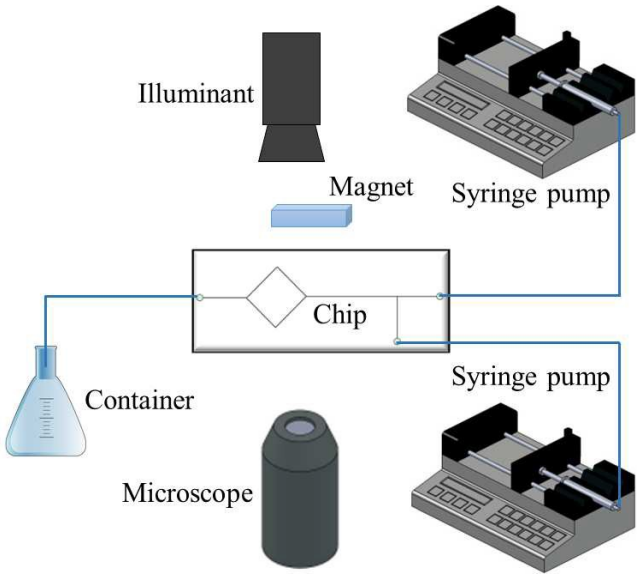

Fig.2 Scheme of the experimental setup. The permanent magnet is added at one side of the microchannel to form non-uniform magnetic field.

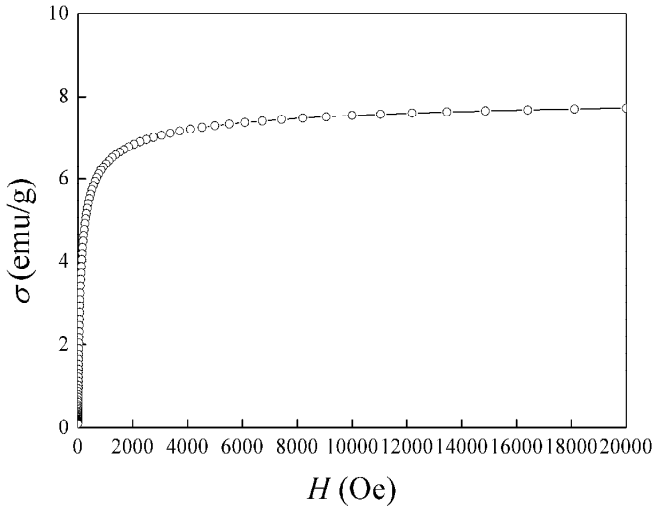

Fig.3 Magnetization curves of the ferrofluid used in our experiments (EMG807, Ferrotech, USA, at 300 K). The data is from the manufacturer's data sheet.

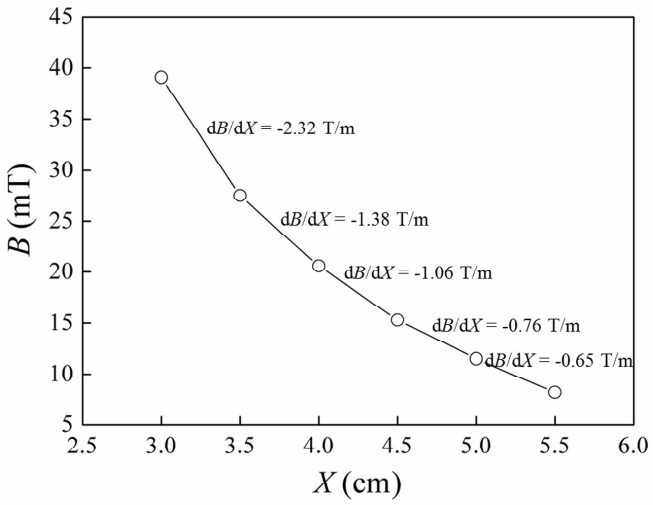

Fig.4 The variation of the magnetic flux density of the permanent magnet with the distance from the centre of the magnet.

2.3 Materials

In order to form ferrofluid droplets, water-based ferrofluid (EMG 807, Ferrotech, USA) and mineral oil (CAS 8042-47-5, Aladdin Industrial Corporation, China) were introduced as the dispersed phase and continuous phase, respectively. The density and viscosity of the ferrofluid were ρ_d = 1,100 kg·m^{-3} and μ_d = 2 mPa·s. As the magnetic particles had an average diameter of 10 nm, the magnetoviscous effect could be negligible. [26] The particles volume concentration was 1.8 % in this ferrofluid with the initial susceptibility χ = 0.39. The mineral oil with 4 % (wt) surfactant sorbitan lauric acid ester (Span20, Tianjin Kemiou Chemical Reagent Co., Ltd, China) was used as the continuous phase. The density and viscosity of the continuous phase were ρ_c = 838 kg·m^{-3} and μ_c = 35 mPa·s, respectively. The interfacial tension between the ferrofluid and mineral oil measured by an interface tensiometry (Dataphysics, Germany) was σ = 1.5 mN·m^{-1}.

In the experiment, the flow rate of Q_d was varied from 0.5 to 1.5 ml·h^{-1}, while the flow rate of Q_c was adjusted between 0.4 and 30 ml·h^{-1}. The corresponding capillary numbers $Ca = u\mu_c/\sigma$ ranges from 0.01 to 0.47, here u is the superficial velocity of the fluid flowing into the Y-junction ($u = (Q_d + Q_c)/w_c^2$) and w_c is the width of the microchannel. Reynolds number $Re = \rho_c w_c u/\mu_c$ ranges from 0.005 to 0.19.

3 Results and discussion

3.1 Breakup of the ferrofluid droplets in the Y-junction

Figure 5 shows the evolution of the ferrofluid droplet at the Y-junction divergence (Q_d = 1 ml·h^{-1}, Q_c = 2 ml·h^{-1}). Fig. 5 (a) and (b) are the symmetrical breakup of the ferrofluid droplet without magnetic field and the asymmetrical breakup of the ferrofluid droplet with magnetic field, respectively.

In the absence of the magnetic field, a build-up of upstream pressure would be created when the ferrofluid droplet arriving at the Y- junction penetrates into the main and branch channels. The droplet neck firstly protrudes towards the direction of main channel when the rear of the droplet entirely enters into the Y-junction. The neck width and the interface curvature of the droplet neck gradually decrease due to the driving of the continuous phase liquid. The two forming daughter droplets further block the flow of the continuous phase in the branch arms, accelerating the build-up of the upstream pressure. When the thin thread decreases up to a certain value, the curving direction of droplet neck reverses and becomes concave. Finally, the droplet rapidly splits into two daughter droplets with identical size because of the symmetric nature of the microchannel configuration and the flow field. The similar results were also achieved experimentally and numerically by Yamada *et al.* [22] and Carlson *et al.*,[33] respectively.

In this experiment, the non-uniform magnetic field was attained by placing one permanent magnet on the side of the upper arm. When the mother droplet flows into the Y-junction, the forefront of droplet prefers to extend in the upper arm due to the

strong magnetic attraction. The size of the daughter droplet in the upper arm gradually increases with the continuous injection of liquid, enhancing the action of magnetic force as the body force. [27] Under such non-uniform magnetic field, the magnetic force acting on the droplet is not symmetrical, resulting in the obvious difference of the interface deformation on the droplet neck with and without the magnetic field between Fig. 5 (a) and (b), respectively. Eventually, the mother droplet generates the asymmetric breakup and a comparatively bigger droplet is formed in the upper arm.

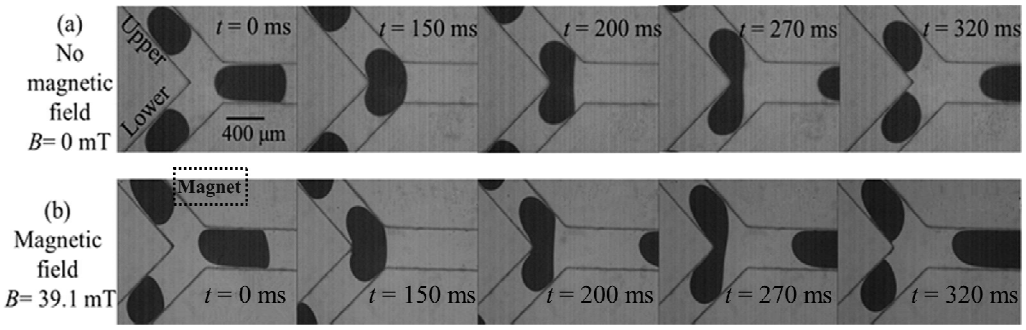

Fig.5 Temporal evolution of the breakup of ferrofluid droplets at the Y-junction divergence (Q_d = 1 ml·h^{-1}, Q_c = 2 ml·h^{-1}). The dotted box indicates the magnet on the side of the upper arm.

In order to study the influence of flow rate ratio Q_d/Q_c on the breakup of ferrofluid droplets, a series of experiment were carried out to investigate the distribution behaviors of ferrofluid droplets under various flow rate ratios. Fig. 6 (a) and (b) show the symmetrical distribution without magnetic field and the asymmetrical distribution with magnetic field (B = 39.1 mT), respectively. It could be found that the size of the mother droplet decreases with the decreases of flow rate ratio Q_d/Q_c. This is mainly because Q_d/Q_c determines the volume of the mother droplet at the upstream

T-junction[12, 34] and the magnetic force changes the symmetrical distribution mode of ferrofluid droplets. The asymmetric degree of droplet size distribution increases with the decrease of Q_d/Q_c. In the following discussion, we would firstly analyze the magnetic-regulatory mechanism of the sizes of daughter droplets.

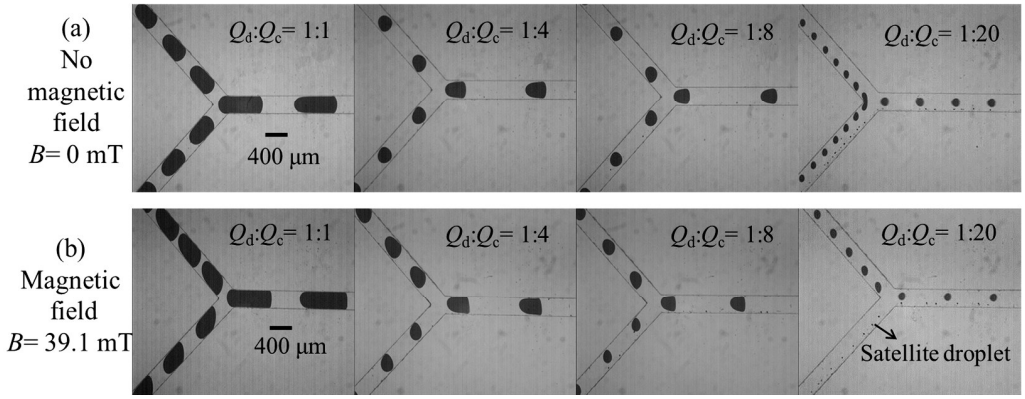

Fig.6 Distribution of the ferrofluid droplets at the Y-junction divergence under various flow rate ratios (Q_d = 1 ml·h^{-1}).

3.2 Magnetic control over the sizes of daughter droplets

Figure 7 shows the volume ratio of the daughter droplets flowing in the upper arm and in the lower arm V_u/V_l as a function of Q_d/Q_c under four different magnetic flux densities. V_u and V_l represent the volumes of the droplet in the upper arm and in the lower arm, respectively. As shown in Fig.7, in the absence of the magnetic field, the symmetrical breakup of ferrofluid droplets occurs in the Y-junction. The volume ratio V_u/V_l is 1, and remains unchanged with the increase of Q_d/Q_c. It consists with the previous results reported by Yamada *et al*. [22] and Carlson *et al*.. [33] Wu et al. [35] found that the feedback effects of asymmetrical collision and staggered flow of bubble pairs

at the T-junction convergence could cause the asymmetric breakup of bubbles at the T-junction divergence, but the loop feedback effect in our experiment is nearly negligible. This is due to that the interfacial tension between the gas and liquid phase in Wu's experiment was larger (σ = 34.3 mN·m^{-1}) and the frontal collisions of bubble pairs at the T-junction convergence was stronger. Differently, in our work, the interfacial tension between the ferrofluid and mineral oil was smaller (σ = 1.5 mN·m^{-1}), the collisions of ferrofluid droplets at the Y-junction convergence was moderate and disenable to bring about the asymmetric accumulation of pressure. The counteractive effect of droplets collision at the Y-junction convergence could be negligible.

In the presence of the external field, V_u/V_l decreases with the increase of Q_d/Q_c and then level off up to 1. It implies that the magnetic field has little influence on V_u/V_l at a higher Q_d/Q_c. This is because when Q_d/Q_c exceeds 1, the length of the mother droplet l_0 is greater than the width of the microchannel w_c. When the mother droplet arrives at the Y-junction divergence, owing to the slower flow rate of continuous phase, the droplets need much more time to rupture, which leads to a slower growing rate of the droplet volume. In comparison with the fluidic squeezing effect, the influence of the magnetic body force on the sizes of daughter droplets is not significant. Moreover, the forward daughter droplets in the branches always contact with the channel wall and block the branch arms, the magnetic force could hardly provide the confined droplets with additional power for the increase of V_u. However, when Q_d/Q_c is less than 1,

there exists a visible gap between the daughter droplet and the wall, which reduces the upstream pressure in the Y-junction. The unconfined droplets are more convenient to slip into the upper arm to form a relatively bigger daughter droplet due to the magnetic attraction.

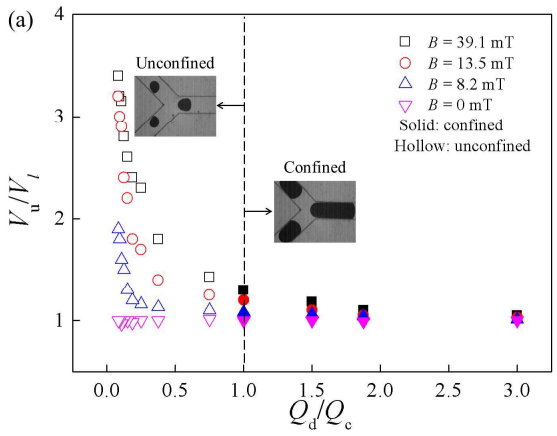

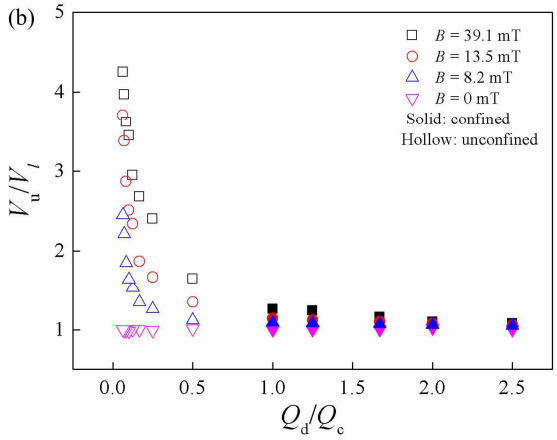

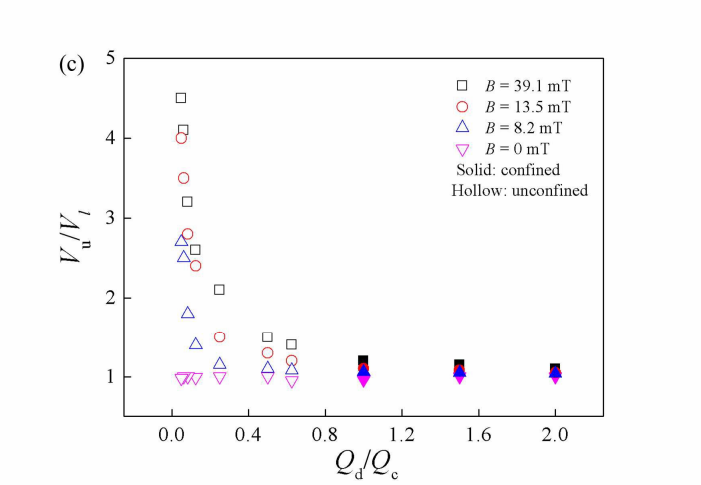

Fig.7 Volume ratio of the daughter droplets flowing in the upper and lower arm V_u/V_l as a function of Q_d/Q_c under four different magnetic flux densities: (a) Q_d = 1.5 ml·h^{-1}, (b) Q_d = 1 ml·h^{-1} and (c) Q_d = 0.5 ml·h^{-1}, respectively. The hollow symbols denote unconfined droplets and the solid symbols denote confined droplets.

In addition, the magnetic force could shift the mass center of mother droplet in the main channel, and sequentially affect its breakup behavior in the downstream Y-junction. This study is mainly focused on the droplets whose forefronts locate at the end of the main channel, as sketched in Fig. 8(a). The mother droplet is divided into two parts through the center line of the main channel oo'. The cross-sectional area of the upper part and the lower part of the mother droplet are marked as S_1 and S_2, respectively. The area ratio S_1/S_2 represents the asymmetric degree of mother droplet distribution stemming from the magnetic attraction. In the absence of the magnetic field, the mother droplet symmetrically distributes on the two sides of the center line of the channel, the area ratio S_1/S_2 is 1. However, in the presence of the magnetic field, the ferrofluid droplet deflects toward the upper-wall with the higher magnetic field

gradient, resulting in the asymmetric distribution of the mother droplet in the main channel. In this study, the asymmetric distribution of mother droplets by the magnetic force is defined as the "initial distribution" of the droplets. It could be clearly seen from Fig. 8(a) that at a given Q_d/Q_c, S_1/S_2 increases gradually with the magnetic flux density, especially at a lower Q_d/Q_c. The higher magnetic field strength could lead to more intensive magnetization of ferrofluid under the larger magnetic field gradient, consequently, a stronger attractive force would be created, which resulted in a noticeable deflection of moving direction of the mother droplets from the original route in the main channel. It indicates that the "initial distribution" of the droplets could remarkably affect the asymmetric breakup process at the downstream Y-junction, i.e., the "secondary distribution". Fig. 8(b) shows the temporal evolution of S_1/S_2 with a magnetic field (B = 39.1 mT). The time zero is set at the moment when the forefront of the droplet exactly locates at the end of the main channel. As the mother droplet gradually flows into the Y-junction, the area ratio S_1/S_2 increases correspondingly, meaning the augment of the asymmetry of "initial distribution". This is mainly because as the droplet penetrates into the Y-junction, the inherent restriction of the wall starts to fall off, thus the ferrofluid droplet has a larger extending space in the direction of the magnetic force. Meanwhile, the asymmetry of "initial distribution" in the main channel enlarges the difference of the magnetic force acting on the upper part and the lower part of mother droplets. Consequently, such a positive feedback effect induced by the magnetic force prompts the asymmetric breakup of ferrofluid droplets.

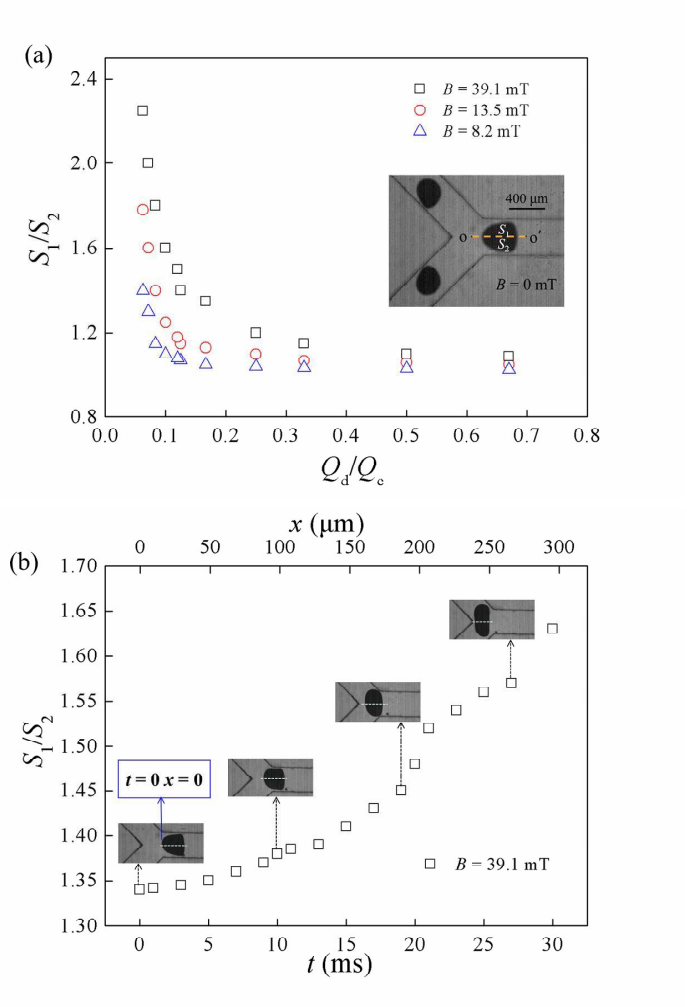

Fig.8 (a) Cross-sectional area ratio of the upper part and the lower part of mother droplets S_1/S_2 as a function of Q_d/Q_c under three different magnetic flux densities (Q_d = 1 ml·h^{-1}). (*Inset*) the flow condition without magnetic field (B = 0 mT, Q_d:Q_c = 1:8). (b) Temporal evolution of S_1/S_2 as a function of time and the forward distance of the droplet with a magnetic field (B = 39.1 mT) and a fixed ratio (Q_d = 1 ml·h^{-1}, Q_c = 8 ml·h^{-1}).

Figure 9 shows the volume of the daughter droplets in the upper and lower arms as a function of magnetic flux density. At a given Q_d/Q_c, V_u increases with the magnetic

flux density, but the opposite trend is found in V_l. This is because the magnetic force promotes the motion of the daughter droplet in the upper arm and the enhancement of the magnetic force could attract more magnetic particles to flow into the upper arm, accordingly they jointly lead to the increase of V_u. Meanwhile, the simultaneously increasing flow resistance with the increase of the droplet size could reduce the flow rate of the continuous phase in the upper arm and accordingly partly counteract the magnetic effect. Especially at the higher total flow rate, the hydrodynamic force would play a dominant role. [31] Therefore, the change of V_u under a stronger magnetic field is not obvious. On the contrary, the magnetic force impedes the motion of daughter droplet in the lower arm, leading to a relatively smaller volume V_l. In addition, the magnetic-induced change of local viscosity [36] and the interfacial slip of the magnetic nanoparticles [37] could also affect the size changes of the daughter droplets.

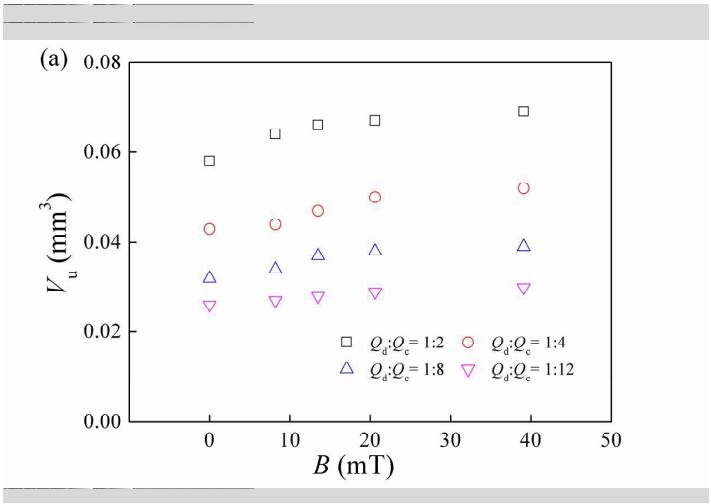

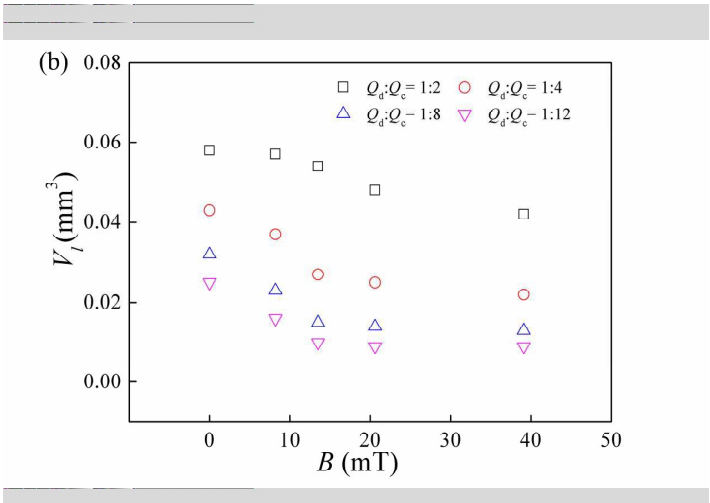

Fig.9 a-b Volume variation of the daughter droplets in the upper and lower arms V_u and V_l with the magnetic flux density, respectively, under four different flow rate ratios (Q_d = 1 ml·h^{-1}).

3.3 Transition between breakup and non-breakup

Whether a droplet at the Y-junction splits or not is a crucial issue for droplet manipulation in the microchannel. Many efforts have been devoted to predict the transition between breakup and non-breakup of the droplets in the literature.[20, 38, 39] Link *et al*. [20] introduced a concept of droplet extension and proposed a correlation for predicting the transition between breakup and non-breakup of the droplets in terms of the classical Rayleigh-Plateau instability. Based on the simple geometric construction for the interfacial shape of droplet and the lubrication analysis in a narrow gap, Leshansky and Pismen [38] found that the flow pattern transition depended mainly on the initial length of droplets and the capillary number *Ca*. Similar experimental observations were also made in both T-junctions and Y- junctions. [32, 40, 41]

It could be found from Fig.6 that in the absence of the magnetic field, the ferrofluid

droplet always generates the symmetrical breakup in the Y-junction, rather than flows into one of its arms with a lower hydrodynamic resistance. [42] Comparing with the usually used T-junction in the literature,[20, 39, 41] the sharp angle at the Y-junction plays an important role in tailoring droplets. The droplet neck thins more rapidly and could reach the critical state for breakup more easily. Finally, the droplet pinches off under the action force from the continuous phase and the counterforce from the sharp angle. However, in the presence of a magnetic field (B = 39.1 mT), the droplet emerges the asymmetric breakup and a bigger daughter droplet is formed in the upper arm. Particularly, when Q_c was increased to 20 ml·h^{-1}, the non-breakup of the droplet was observed: the mother droplets completely flowed into the upper arm, while the undesired satellite droplets generated in the upstream T-junction were completely filtered into the lower arm.

For better understanding the magnetic effect, the flow pattern regime of the breakup and non-breakup under various magnetic flux densities is shown in Fig.10. For system without magnetic field (B = 0 mT), all ferrofluid droplets in the operating regime breakup at the Y-junction divergence and the dimensionless length of the mother droplet l_0/w_c decreases with the increase of capillary number Ca. For system with external magnetic field, the non-breakup behavior of the droplets was observed. The critical capillary number decreases with the increase in the magnetic flux density. For instance, when B increases from 13.5 mT to 39.1 mT, the critical capillary number reduces from 0.42 to 0.31, and the non-breakup flow regime is gradually extended.

Once approaching the transition line, a slight change in droplet size or the capillary number could easily cause the pattern transition of ferrofluid droplets in the Y-junction. As shown in Fig.10, the bigger droplet is more inclined towards breakup and the magnetic force would behave limited regulatory performance on it. On the contrary, when the droplet size is smaller, the magnetic force could play an important role in the pattern transition. Instead of breaking up into two daughter droplets, the whole mother droplet could be controlled to flow into the desired arm. This magnetic control concept facilitates the pattern transition between breakup and non-breakup and provides a new route for the separation of undesired satellite droplets.

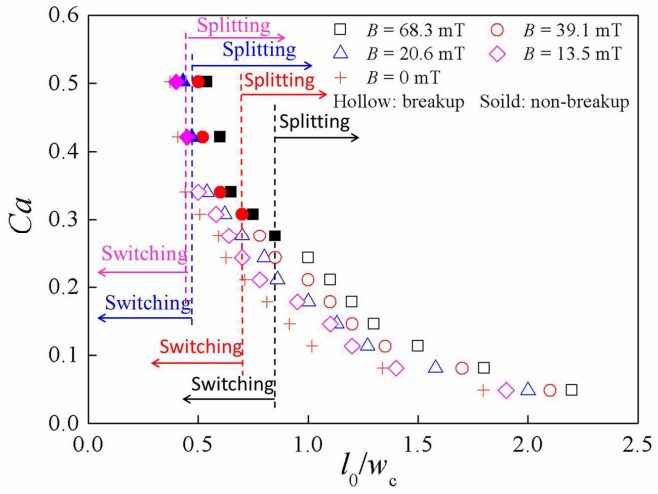

Fig.10 The pattern diagrams for ferrofluid droplet breakup and non-breakup in the Y-junction. The hollow markers denote breakup and the solid markers denote non-breakup. The dashed lines describe the threshold for splitting or switching under different magnetic flux densities.

3.4 Theoretical prediction for the sizes of daughter droplets

Link *et al*. [20] implemented a pioneer work for the precise manipulation of the sizes of daughter droplets in the T-junction by adjusting the length ratio of the two daughter arms. In analogy with the electric-current-splitting device, they found that the ratio of volumes of the two daughter droplets is proportional to the ratio of volumes flow rates but inversely to the ratio of sidearm lengths. Bedram and Moosavi [43] numerically investigated the breakup of droplets in an asymmetric T junction consisting of an inlet channel and two different-width outlet channels. Simulated results indicate that the volume ratio of the droplet in the obstruction breakup regime could be described in terms of a power law function of channel width ratio,

$$V_1 / V_2 = a(w_1 / w_2)^b \tag{2}$$

Where a, b are fitting parameter and depend on the capillary number *Ca*. Similarly, Samie *et al*. [44] utilized the asymmetric T-junctions with two branches of identical lengths but different cross sections of equilateral-triangle for generating unequal-sized microdroplets. They deduced the volume ratio of daughter droplets V_1/V_2 for branch widths of w_1 and w_2 as

$$V_1 / V_2 = (w_1 / w_2)^4 \tag{3}$$

More recently, Wang and Yu [45] investigated the asymmetric breakup of a droplet suspended in an axisymmetric extensional flow through the volume of fluid (VOF) method. Based on a comprehensive analysis of hydrodynamic regimes, they proposed a simple model to predict the volume ratio $r_s = V_B / V_S$ of daughter droplets (the subscripts *B* and *S* stand for the bigger and smaller droplets, respectively),

$$r_s = r_0 + \frac{e \times (A_s)^b}{(Ca - Ca_c)^c} \tag{4}$$

where e, b and c are parameters fitted from data of numerical calculations, $A_s = l - s / l + s$ is defined as the asymmetry of the flow field (l and s are the distances of the right and left end of the droplet from the center of the device, respectively), Ca_c is the critical capillary number to determine whether the droplet will break up or not and could be obtained from the fitting curves, the initial volume ratio r_0 is a function of A_s and could be calculated by

$$r_0 = \frac{-(A_s)^3 + 3A_s + 2}{(A_s)^3 - 3A_s + 2} \tag{5}$$

In order to accurately predict the sizes of the daughter droplets in the Y-junction with the magnetic field, in this paper, the magnetic Bond number is adopted to represent the ratio between the magnetic force and the surface tension, $Bo_m = \mu_0 \chi w_c H^2 / \sigma$.[27] When B rises from 8.2 mT to 39.1 mT, Bo_m increases from 5.6 to 126.6. Taking the influence of the hydrodynamic force and magnetic force on the sizes of daughter droplets into account, a correlation of V_u/V_l to Q_d/Q_c, Ca and Bo_m could be attained by the fitting experimental data

$$V_u / V_l = 1 + 0.05(Q_d / Q_c)^{-0.95} (Ca)^{0.06} (Bo_m)^{0.38} \tag{6}$$

It could be seen from Eq.6 that V_u/V_l increases with either the decrease in Q_d/Q_c or the increase of Bo_m, and the influence of Q_d/Q_c on V_u/V_l is more sensitive than that of B. This is because the volume of the mother droplet at the upstream T-junction is primarily determined by the flow rate ratio,[12, 34] which dramatically affects the magnetic manipulation of both "initial distribution" and "secondary distribution". In the range of present experiments, the capillary numbers Ca has inapparent influence

on V_u/V_l. The mean relative deviation of the correlation is 5.25% as shown in Fig.11 ($0.03 < Q_d/Q_c < 3$, $0.01 < Ca < 0.28$, $0 < Bo_m < 126.6$). It indicates that by adjusting the fluid flow rate and the magnetic flux density, we could obtain the desirable sizes of ferrofluid droplets in the microchannel.

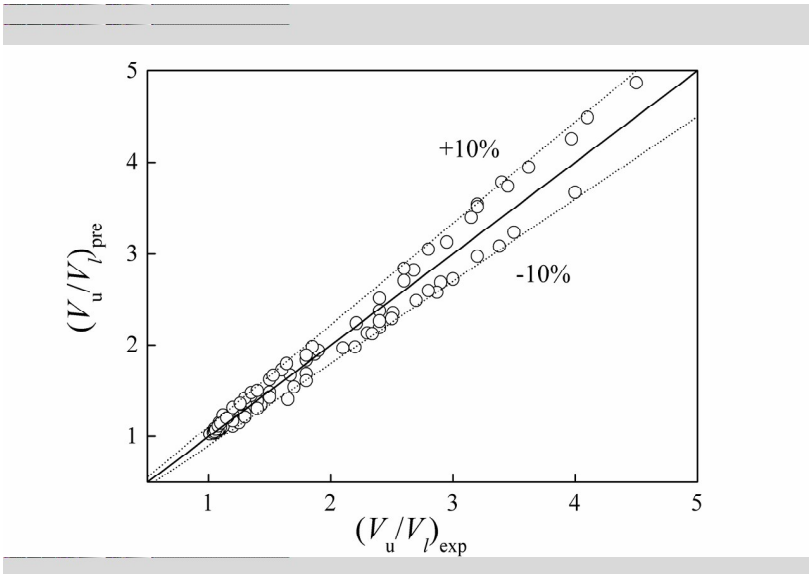

Fig.11 Comparison of the volume ratios V_u/V_l between the predicted values from Eq.5 and the experimental data from our experiment.

4 Conclusion

In this study, we present a magnetofluidic control technique for manipulating the breakup of ferrofluid droplets in a microfluidic Y-junction. The controllable manipulation was achieved by using the neodymium iron boron (NdFeB) magnet to induce the asymmetric breakup of ferrofluid droplets in the symmetrical channel. This method could tailor a mother droplet into two daughter droplets of desirable sizes or switch the droplet entirely into an expected arm. The magnetic force could shift the

mass center of mother droplet in the main channel and sequentially affect its breakup behavior in the downstream Y-junction, as the magnetic-induced "initial distribution" of the droplet promotes its asymmetric breakup at the Y-junction. In the presence of the magnetic field, the magnetic force prompts the movement of the daughter droplet in the upper arm, whereas it impedes the growth of the daughter droplet in the lower arm. V_u/V_l increases with the decrease of Q_d/Q_c or the increase of B. A correlation for predicting the V_u/V_l was proposed by means of the Q_d/Q_c, Ca and Bo_m. Moreover, the combined effect of the magnetic force and the hydrodynamic force facilitates the pattern transition between breakup and non-breakup of the ferrofluid droplets. These favorable results show that the active and exquisite control by the magnetic force could produce the ferrofluid emulsions with desirable sizes. This work also provides a new avenue to explore complex interfacial phenomena.

Acknowledgments

The financial supports for this study from the National Nature Science Foundation of China (No.21276175, 91434204, 21106093), the Tianjin Natural Science Foundation (13JCQNJC05500), the aid of Opening Project of State Key Laboratory of Chemical Engineering (No.SKL-ChE-13T04) and the Programs of Introducing Talents of Discipline to Universities (Grant No.B06006) are gratefully acknowledged.

References

1. G. M. Whitesides, *Nature*, 2006, **442**, 368-373.
2. S. Y. Teh, R. Lin, L. H. Hung and A. P. Lee, *Lab on a chip*, 2008, **8**, 198-220.

3. S. Marre and K. F. Jensen, *Chemical Society reviews*, 2010, **39**, 1183-1202.
4. M. A. Gijs, F. d. r. Lacharme and U. Lehmann, *Chemical reviews*, 2009, **110**, 1518-1563.
5. K. Zhang, Q. Liang, X. Ai, P. Hu, Y. Wang and G. Luo, *Lab on a chip*, 2011, **11**, 1271-1275.
6. H. Song, D. L. Chen and R. F. Ismagilov, *Angewandte Chemie International Edition*, 2006, **45**, 7336-7356.
7. N.-T. Nguyen and M.-F. Chai, *Micro and Nanosystems*, 2009, **1**, 17-21.
8. M. A. Gijs, *Microfluidics and Nanofluidics*, 2004, **1**, 22-40.
9. J. Liu, S.-H. Tan, Y. Yap, M. Ng and N.-T. Nguyen, *Microfluidics and Nanofluidics*, 2011, **11**, 177-187.
10. J. Liu, Y. F. Yap and N.-T. Nguyen, *Physics of Fluids (1994-present)*, 2011, **23**, 072008.
11. I. Torres-Díaz and C. Rinaldi, *Soft matter*, 2014, **10**, 8584-8602.
12. P. Garstecki, M. J. Fuerstman, H. A. Stone and G. M. Whitesides, *Lab on a chip*, 2006, **6**, 437-446.
13. T. Fu, D. Funfschilling, Y. Ma and H. Z. Li, *Microfluidics and Nanofluidics*, 2010, **8**, 467-475.
14. L. Salkin, A. Schmit, L. Courbin and P. Panizza, *Lab on a chip*, 2013, **13**, 3022-3032.
15. H. Gu, C. U. Murade, M. H. G. Duits and F. Mugele, *Biomicrofluidics*, 2011, **5**, 011101.
16. Y. Wu, T. Fu, Y. Ma and H. Z. Li, *Soft Matter*, 2013, **9**, 9792-9798.
17. L. Schmid and T. Franke, *Applied Physics Letters*, 2014, **104**, 133501.
18. C. A. Stan, S. K. Y. Tang and G. M. Whitesides, *Analytical chemistry*, 2009, **81**, 2399-2402.
19. A. R. Abate, M. B. Romanowsky, J. J. Agresti and D. A. Weitz, *Applied Physics Letters*, 2009, **94**, 023503.
20. D. Link, S. L. Anna, D. Weitz and H. Stone, *Physical review letters*, 2004, **92**, 054503.
21. L. Salkin, L. Courbin and P. Panizza, *Physical Review E*, 2012, **86**, 036317.
22. M. Yamada, S. Doi, H. Maenaka, M. Yasuda and M. Seki, *Journal of colloid and interface science*, 2008, **321**, 401-407.
23. D. R. Link, E. Grasland‐Mongrain, A. Duri, F. Sarrazin, Z. Cheng, G. Cristobal, M. Marquez and D. A. Weitz, *Angewandte Chemie International Edition*, 2006, **45**, 2556-2560.
24. Y.-F. Yap, S.-H. Tan, N.-T. Nguyen, S. S. Murshed, T.-N. Wong and L. Yobas, *Journal of Physics D: Applied Physics*, 2009, **42**, 065503.
25. Y. N. Cheung and H. Qiu, *Physical Review E*, 2011, **84**, 066310.
26. N. Pamme, *Lab on a chip*, 2006, **6**, 24-38.
27. N.-T. Nguyen, *Microfluidics and nanofluidics*, 2012, **12**, 1-16.
28. N.-T. Nguyen, K. M. Ng and X. Huang, *Applied Physics Letters*, 2006, **89**, 052509.

29. T. Say-Hwa, N. Nam-Trung, Y. Levent and K. Tae Goo, *Journal of Micromechanics and Microengineering*, 2010, **20**, 045004.
30. S. H. Tan and N.-T. Nguyen, *Physical Review E*, 2011, **84**, 036317.
31. Y. Wu, T. Fu, Y. Ma and H. Li, *Microfluidics and Nanofluidics*, 2015, **18**, 19-27.
32. L. Ménétrier-Deremble and P. Tabeling, *Physical Review E*, 2006, **74**, 035303.
33. A. Carlson, M. Do-Quang and G. Amberg, *International Journal of Multiphase Flow*, 2010, **36**, 397-405.
34. G. F. Christopher, N. N. Noharuddin, J. A. Taylor and S. L. Anna, *Physical Review E*, 2008, **78**, 036317.
35. Y. Wu, T. Fu, C. Zhu, Y. Lu, Y. Ma and H. Z. Li, *Microfluidics and Nanofluidics*, 2012, **13**, 723-733.
36. C. Flament, S. Lacis, J. C. Bacri, A. Cebers, S. Neveu and R. Perzynski, *Physical Review E*, 1996, **53**, 4801-4806.
37. S. M. S. Murshed, S. Tan, N. Nguyen, T. Wong and L. Yobas, *Microfluidics and Nanofluidics*, 2009, **6**, 253-259.
38. A. Leshansky and L. Pismen, *Physics of Fluids (1994-present)*, 2009, **21**, 023303.
39. X. Wang, C. Zhu, T. Fu and Y. Ma, *Chemical Engineering Science*, 2014, **111**, 244-254.
40. B. Eshpuniyani, J. B. Fowlkes and J. L. Bull, *International Journal of Heat and Fluid Flow*, 2005, **26**, 865-872.
41. T. Fu, Y. Ma, D. Funfschilling and H. Z. Li, *Chemical Engineering Science*, 2011, **66**, 4184-4195.
42. P. Parthiban and S. A. Khan, *Lab on a chip*, 2012, **12**, 582-588.
43. A. Bedram and A. Moosavi, *The European Physical Journal E*, 2011, **34**, 1-8.
44. M. Samie, A. Salari and M. B. Shafii, *Physical Review E*, 2013, **87**, 053003.
45. J. Wang and D. Yu, *Microfluidics and Nanofluidics*, 2015, **18**, 709-715.

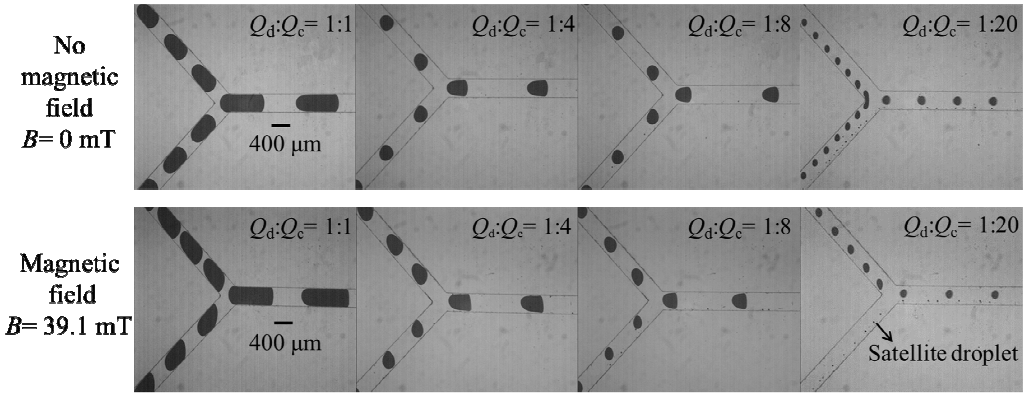

Breakup of the ferrofluid droplets at the Y-junction divergence under various flow rate ratios.